SSC Trigger Cross Sections

Frank E. Paige

Physics Department
Brookhaven National Laboratory
Upton, NY 11973

Most triggers at the SSC will involve multiple jets or jets plus leptons or missing p_T; cross sections for these are calculated. Events containing W^+W^- pairs will be an important signature at the SSC and provide a good test of its trigger system. Properties of such events are given.

At $\sqrt{s} = 40\,\text{TeV}$ and $L = 10^{33}\,\text{cm}^{-2}\text{sec}^{-1}$ the SSC will produce over 10^8 interactions per second. The trigger system must reduce this rate to a few events per second to be recorded for later analysis. Presumably at least the initial stages of the trigger must be based on a few simple quantities, such as:

- Total transverse energy.
- Number and transverse energies of jets.
- Number and transverse momenta of charged leptons.
- Amount of missing p_T.

More sophisticated quantities might be considered at a later stage. This note contains calculations of some standard model cross sections for combinations of jets and leptons. These cross sections will probably dominate the trigger rate, and they represent potential backgrounds for any new physics signature.

The calculations are mainly based on ISAJET 5.02, which is identical to Version 5.00[1] except for the correction of several errors. ISAJET simulates pp and $\bar{p}p$ interactions at high energies. Primary partons are generated according to leading-log QCD cross sections, leading-log QCD radiation from initial and final partons is produced, the resulting partons are fragmented independently, and beam jets based on minimum bias data are added. These events have been analysed with a trivial calorimeter simulation (CALSIM) having uniform cells with $\Delta y = .1$ and $\Delta\phi = 5°$. The energy of each particle is completely confined to a single cell but is smeared with the resolutions

$$\frac{\Delta E}{E} = \frac{.15}{\sqrt{E}} \qquad \text{for electrons and photons}$$

$$\frac{\Delta E}{E} = \frac{.35}{\sqrt{E}} \qquad \text{for hadrons}$$

Jets have been found by an algorithm (GETJET) which clusters all cells which have transverse energy greater than 0.5 GeV and which are within a given radius

$$\Delta R = \left[(\Delta y)^2 + (\Delta\phi)^2\right]^{1/2}.$$

For $\Delta R = 1.0$ this is essentially equivalent to the UA1 jet algorithm. Both CALSIM and GETJET are contained in the ISAJET PAM.

New heavy particles will generally be produced with transverse momenta comparable to their masses, so if they decay into several quarks or gluons, they will give rise to multijet final states. Multiple jets can also be produced by higher order QCD processes, which are approximated in ISAJET by two-body QCD hard scattering combined with leading-log QCD radiation from initial and final state partons. To estimate these cross sections, ISAJET jet events were generated with the primary p_T between 50 GeV and 3200 GeV, and the jets were found with GETJET using various values of ΔR. Figs. 1-3 show the cross sections for 1, 2, 3, 4, 5, and 6 jets with $\Delta R = 1.0$, 0.5, and 0.2 respectively as functions of the minimum E_T for any of the jets. As expected, smaller values of ΔR give smaller cross sections for 1 and 2 jets, since a smaller fraction of the jet energy is included; they give larger cross sections for many jets, since the renormalization group structure of QCD leads to a splitting of jets into closely clustered multiple jets. While multiple jets are suppressed by powers of α_s, most of the decrease of σ with the number of jets comes from the increased total transverse energy of the event. Note that the cross section for jets with $E_T = 1\,\text{TeV}$ is of order 1 nb, corresponding to a rate of 1 per second at full luminosity. Hence a simple transverse energy trigger is sufficient at the highest masses but not for much of the interesting physics beyond the range of the Tevatron.

New particles are often characterized by decays involving jets and charged leptons or missing p_T. Real backgrounds for such signatures can arise from the semileptonic decays of heavy quarks. It is found that the dominant real background comes from decays of c, b, and t quarks produced in gluon jets by the QCD radiation.[2] Production of heavy flavors is still perturbative, but because the gluon cross section is so large, the higher order processes, e.g.

$$g + g \rightarrow q + \bar{q} + g$$

dominate over the lowest order process

$$g + g \rightarrow q + \bar{q}.$$

To estimate such cross sections, a sample of 24000 ISAJET jet events with p_T ranging from 50 GeV to 6400 GeV has been generated. This sample includes both the lowest order processes and higher order ones from the leading-log QCD jet evolution. Events have been rejected if after the QCD jet evolution there is no heavy quark with $p_{T,\,\text{quark}}/p_{T,\,\text{jet}} > .1$ or if after the jet fragmentation there is no $e^{\pm}$, $\mu^{\pm}$, or neutrino with $p_{T,\,\text{lepton}}/p_{T,\,\text{jet}} > .1$. Fig. 4 shows the resulting differential cross sections for $e^{\pm}$ and $\mu^{\pm}$ as a function of the p_T of the lepton. No lepton isolation cuts have been imposed. Fig. 5 shows the corresponding cross section for neutrinos.

Fig. 6 shows the cross sections for an $e^{\pm}$ or a $\mu^{\pm}$ plus 1, 2, 3, 4, 5, and 6 jets as functions of the common minimum E_T for both the lepton and a jet. Obviously, taking the jet and lepton thresholds to be equal is only one possible choice for a trigger, and other choices might be more appropriate for particular new particles. Again these cross sections are based on QCD jet events containing semileptonic decays of heavy quarks, and no lepton isolation criteria are imposed. Note that the lepton is counted as part of a jet,

so that the 1-jet and 2-jet cross sections are virtually indistinguishable. Fig. 7 shows the corresponding cross sections for a neutrino and jets.

This sample took about 1.5 hours to generate on a CDC 7600. Hence the events which survive the cuts have been saved on a CDC format 6250 bpi tape, and an equivalent VAX tape has been made, so that this event sample can be used for further analysis either on a CDC or on a VAX.

Events containing leptons and jets can also arise from the production of W bosons, especially at high p_T. While the W cross section is smaller by a factor of α/α_s than the jet one, the events are more likely to contain hard leptons. To obtain these cross sections a sample of $W^\pm +$ jet events has been generated with $p_{T,W}$ ranging from 50 GeV to 3200 GeV. The differential p_T distribution for $e^\pm$ and $\mu^\pm$ from these events is shown in Fig. 8, and the same distribution for neutrinos is shown in Fig. 9. The cross sections for from 1 to 6 jets plus an $e^\pm$ or a $\mu^\pm$ all above a given E_T are shown in Fig. 10, and the same cross sections with a neutrino instead of a charged lepton are shown in Fig. 11. Evidently the QCD jet and the $W^\pm +$ jet processes are comparable, so that both must be considered.

WW pairs will be one of the most important signatures at the SSC, being the dominant decay mode for a heavy Higgs boson and closely related to the physics of spontaneous symmetry breaking. WW pairs are also a signature of particular relevance to triggering questions, since the cross section is so small that high luminosity is needed even at low masses.

The mode $Z^0Z^0 \to \ell^+\ell^-\ell^+\ell^-$ has very little background but a very small branching ratio. The mode $W^\pm W^\mp \to \ell^\pm \nu \bar{q} q'$ has a combined branching ratio of 25% if both $e^\pm$ and $\mu^\pm$ are included, but the background from $W^\pm$ plus two jets has recently been calculated and is large.[3] For $p_{T,W} \gg m_W$ this background should be reasonably described by the final state branching approximation, since the two jets are nearly collinear. A previous analysis[4] found that the background for $p_{T,W} = 500$ GeV could be reduced to of order the signal by a complicated set of cuts. The most important cut is that on the reconstructed mass for $W \to \bar{q}q'$, but cuts on the shape of the jet-jet system are also essential.

The analysis in Ref. 4 was based on the old version of ISAJET, which did not include initial state gluon radiation. Initial state radiation produces additional low-p_T particles under the jet and so will degrade the W mass resolution. Initial state radiation also generates new background processes like

$$g + g \to W^\pm + \bar{q} + q'$$

and so should reproduce the full background calculation[3] at least qualitatively; no quantitative comparison has yet been made. It is important to study this background in much more detail. For now only the signal

$$\begin{aligned} q + \bar{q} &\to W^\pm + W^\mp, \\ W^\pm &\to e^\pm + \nu, \\ W^\mp &\to \bar{q}' + q'', \end{aligned}$$

is considered. Two samples of 500 events each have been generated with ISAJET 5.02 at $\sqrt{s} = 40\,\text{TeV}$:

- $100\,\text{GeV} < p_{T,W} < 110\,\text{GeV}$ $\quad (M_{WW} \sim 250\,\text{GeV})$
- $500\,\text{GeV} < p_{T,W} < 550\,\text{GeV}$ $\quad (M_{WW} \sim 1000\,\text{GeV})$

The low-p_T sample is of interest for the trigger, while the high-p_T one is directly comparable with the analysis in Ref. 4. The cross sections for these limited regions of p_T are .48 pb and .006 pb respectively.

Fig. 12 shows the p_T distribution for the $e^{\pm}$, and Fig. 13 shows that for the ν in the low-p_T sample. Note that because of the $W^{\pm}$ polarization the electron has an average p_T of only 48 GeV while the neutrino has an average p_T of 76 GeV. The threshold on the p_T of the electron must be set at about 25 GeV to see most of the cross section and, more importantly, to be able to extract the $W^{\pm}$ polarization. This polarization is an important handle on the source of the WW pair.[5] It can be determined from the distribution of the ratio of the $e^{\pm}$ and ν transverse momenta, but only if this distribution is measured over a reasonable fraction of the allowed range.

A trigger requiring just an electron with $p_T > 25\,\text{GeV}$ is clearly too loose; for example the inclusive cross section for $W^{\pm} \to e^{\pm}\nu$ is about 15 nb.[6] It is at least necessary to measure the missing transverse momentum and to reconstruct the transverse momentum of the $W^{\pm}$. A detailed study of missing p_T resolution requires a full detector simulation, but the rapidity coverage needed can be estimated using the trivial simulation CALSIM described above. From Fig. 14 it appears that $|y| < 5$ is sufficient to measure the signal; whether it is also sufficient to suppress the backgrounds requires more study. The transverse mass M_T reconstructed with the trivial calorimeter simulation is shown in Fig. 15. While there is a long tail at high M_T due to extra neutrinos from the decay of the other W, the Jacobean peak is quite pronounced.

Isolation is important both to identify the $e^{\pm}$ and to know that it came from a $W^{\pm}$ rather than from the semileptonic decay of a heavy quark. Fig. 16 shows that almost all of the electrons in the low-p_T sample have less than 5 GeV of extra transverse energy in a cone $\Delta R < .5$ around the electron; the isolation for the high-p_T sample is similar. The few events with large E_T in the cone presumably have extra jets from the initial state gluon radiation. An isolation cut could also be used to separate neutrinos from $W^{\pm}$ decay from those from heavy quark decay. About 55% of the events in the low-p_T sample have no jet above 10 GeV within $\Delta\phi < 30°$ of the missing $\vec{p}_T$.

The inclusive cross section for $W^{\pm} \to e^{\pm}\nu$ with $p_{T,W} > 100\,\text{GeV}$ is about .65 nb, so except for very low mass WW pairs there is no need to reconstruct the $W^{\mp} \to \bar{q}q'$ decay in the trigger. But this reconstruction is crucial to separating the $W^{\pm}W^{\mp}$ signal from the much larger background of $W^{\pm}$ + jets. The resolution on the $W^{\mp}$ mass from clustering effects should at least approximately add in quadrature with the resolution from detector effects, which was studied in detail previously.[4] Therefore, detector effects will be ignored here. The trivial calorimeter simulation CALSIM is used only to provide input for the jet-finding algorithm. Then all particles except neutrinos in a cone $\Delta R < 1$ around the jet axis and with p_T above some minimum threshold are summed with perfect resolution. For the low-p_T sample the jet-finding algorithm almost always finds two jets from $W^{\mp} \to \bar{q}q'$. The best threshold is about .5 GeV. The mass reconstructed with this threshold and perfect resolution for the two highest-p_T jets with $\Delta\phi > 90°$ from the W direction is shown in Fig. 17. While there is a peak at the W mass, it is not very narrow. It must be stressed,

however, the analysis has not been optimized; one could try to find a better clustering algorithm or a better way to select the jets. For the high-p_T sample the jet algorithm almost always finds a single jet. The best cut is about 1 GeV, and with this cut the reconstructed $W^{\mp} \to \bar{q}q'$ mass, Fig. 18, shows a clean peak with a full width of less than 4 GeV. This is considerably narrower than the peak found in Ref. 4 including detector effects but not initial state gluon radiation. In this case the detector effects dominate, so the previous conclusions remain approximately valid.

The $W^{\pm}W^{\mp}$ mass can be reconstructed by a 0C fit, solving for $\vec{p}_\nu$ using the two measured components of the missing $\vec{p}_T$ and the W mass. This generally gives two solutions for each event, although sometimes there is no solution because of additional missing p_T from other neutrinos. (For $W^{\pm} \to e^{\pm}\nu$ at the S$\bar{p}$pS, one solution is often unphysical, but at the SSC the energy is so much greater than the mass that both are usually allowed.) The difference between the generated mass and the reconstructed mass is shown in Fig. 19 for the low-p_T sample and in Fig. 20 for the high-p_T sample. Both plots include only those events which have a consistent solution for $W^{\pm} \to e^{\pm}\nu$ and have a reconstructed $W^{\mp} \to \bar{q}q'$ mass within 20 GeV of the W mass. At least for the high-p_T sample the resolution is smaller than the width of any expected structure.

It is important to decide whether $W^{\pm}W^{\mp}$ pairs can be separated from the background of $W^{\pm}$ + jets. If not, then the only way to address an important part of SSC physics is through $Z^0Z^0 \to \ell^+\ell^-\ell^+\ell^-$, and for high masses this requires an integrated luminosity greater than 10^{40}cm^2. My guess is that the signal can be extracted, at least for high masses, but much more work is needed.

I wish to thank Serban Protopopescu and Gordon Kane for many helpful discussions. This work is supported in part by the United States Department of Energy under contract DE-AC02-76CH00016.

References

1. F.E. Paige and S.D. Protopopescu, ISAJET: A Monte Carlo Event Generator for pp and $\bar{p}p$ Interactions, BNL-37066 (1985).
2. S.H. Aronson, L.S. Littenberg, F.E. Paige, I. Stumer, and D.P. Weygand, in *Proceedings of the 1982 Summer Study on Elementary Particle Physics and Future Facilities*, (Snowmass, CO, 1982), p. 505.
3. J.F. Gunion, Z. Kunszt, and M. Soldate, SLAC-PUB-3709 (1985); S.D. Ellis, R. Kleiss, and W.J. Stirling, CERN-TH-4209 (1985).
4. E. Fernandez, P.D. Grannis, S.L. Linn, J.M. Hauptman, F.E. Paige, and W. Selove, in *Proceedings of the 1984 Summer Study on Elementary Particle Physics and Future Facilities*, (Snowmass, CO, 1982), p. 107.
5. M.J. Duncan, G.L. Kane, and W.W. Repko, Phys. Rev. Letters 55, 773 (1985); G.L. Kane, these proceedings.
6. E. Eichten, I. Hinchliffe, K. Lane, and C. Quigg, Rev. Mod. Phys. 56, 579 (1984).

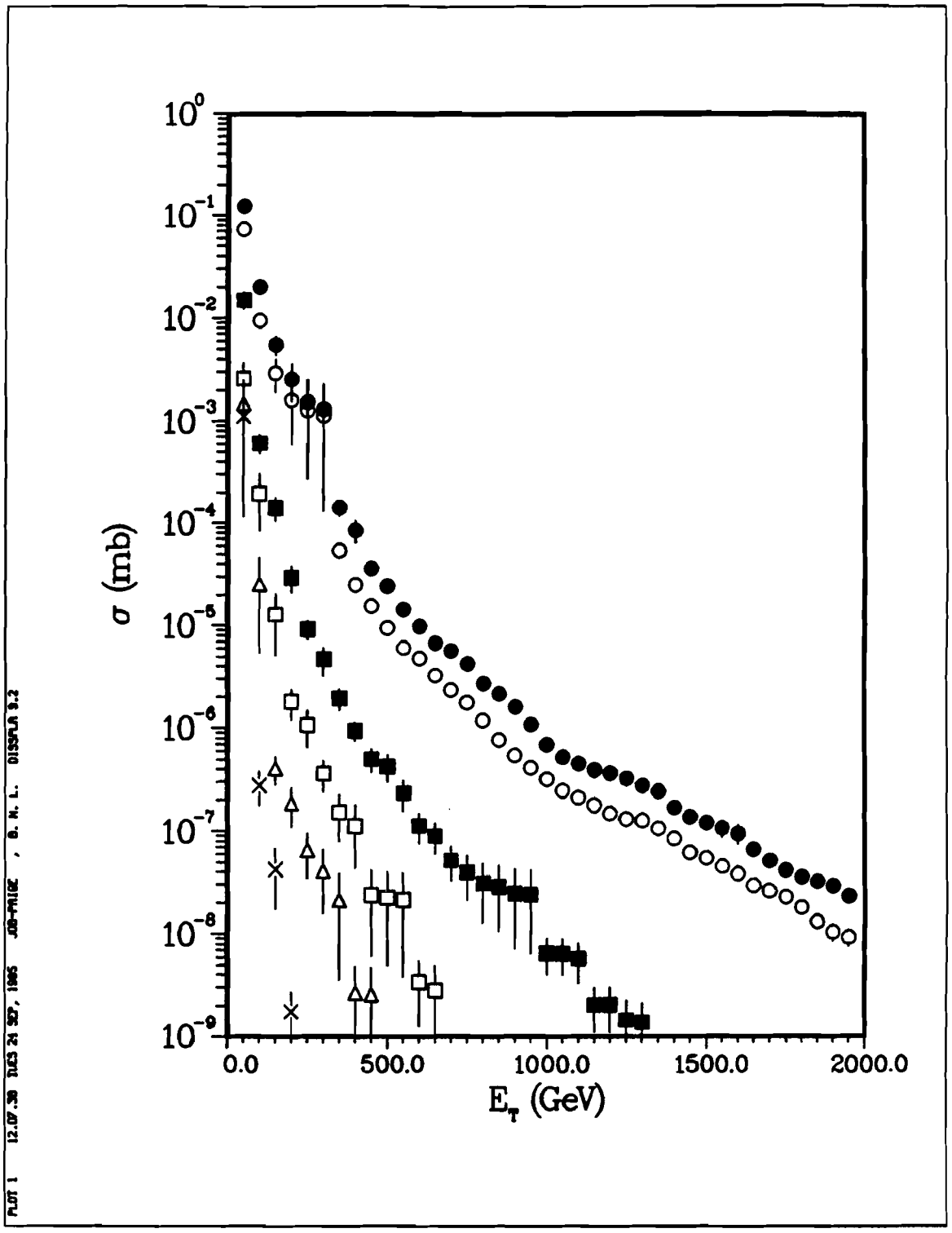

Fig. 1: Cross sections for 1, 2, 3, 4, 5, and 6 jets vs. the minimum E_T of a jet, using $\Delta R = 1.0$ for the clustering.

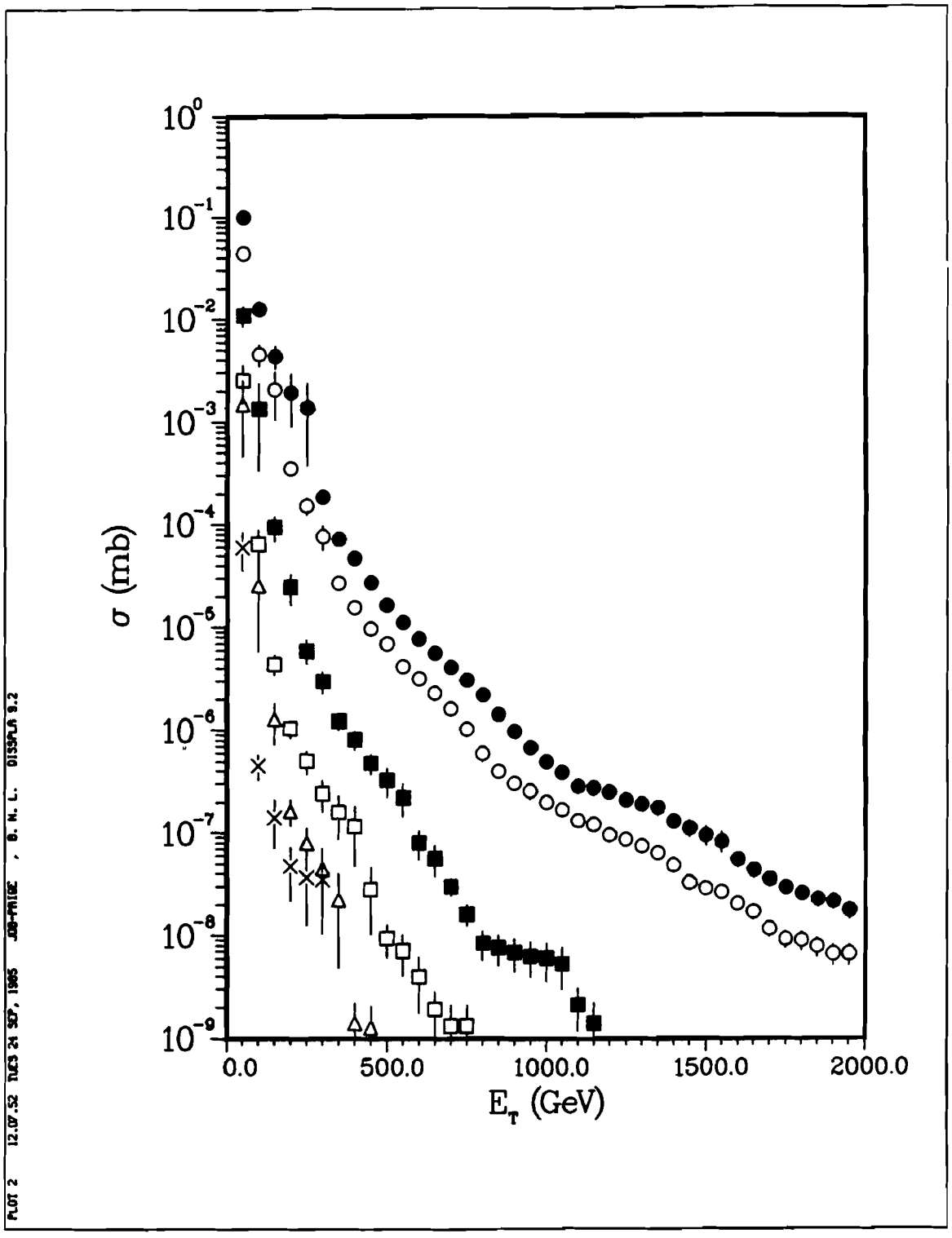

Fig. 2: Cross sections for 1, 2, 3, 4, 5, and 6 jets vs. the minimum E_T of a jet, using $\Delta R = 0.5$ for the clustering.

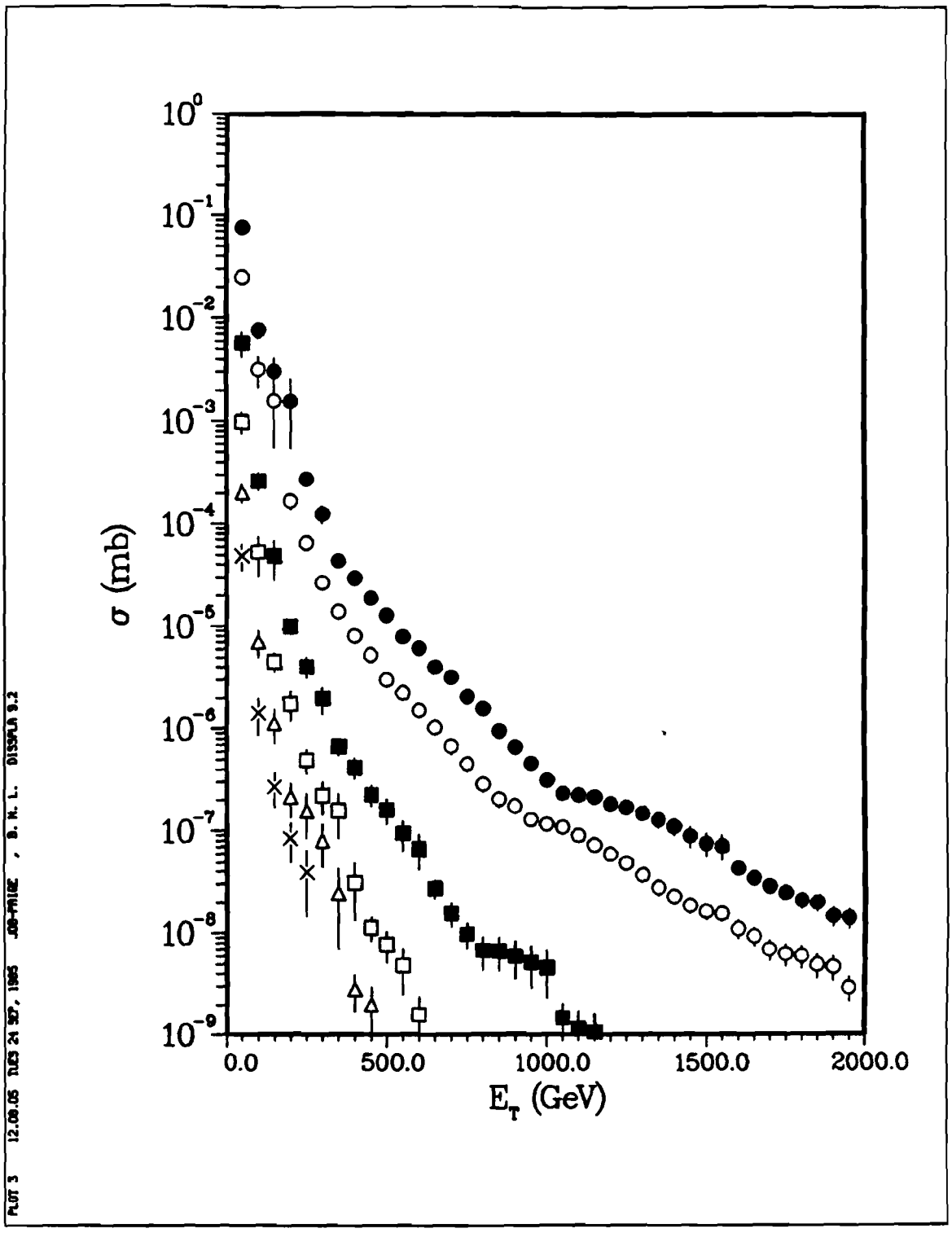

Fig. 3: Cross sections for 1, 2, 3, 4, 5, and 6 jets vs. the minimum E_T of a jet, using $\Delta R = 0.2$ for the clustering.

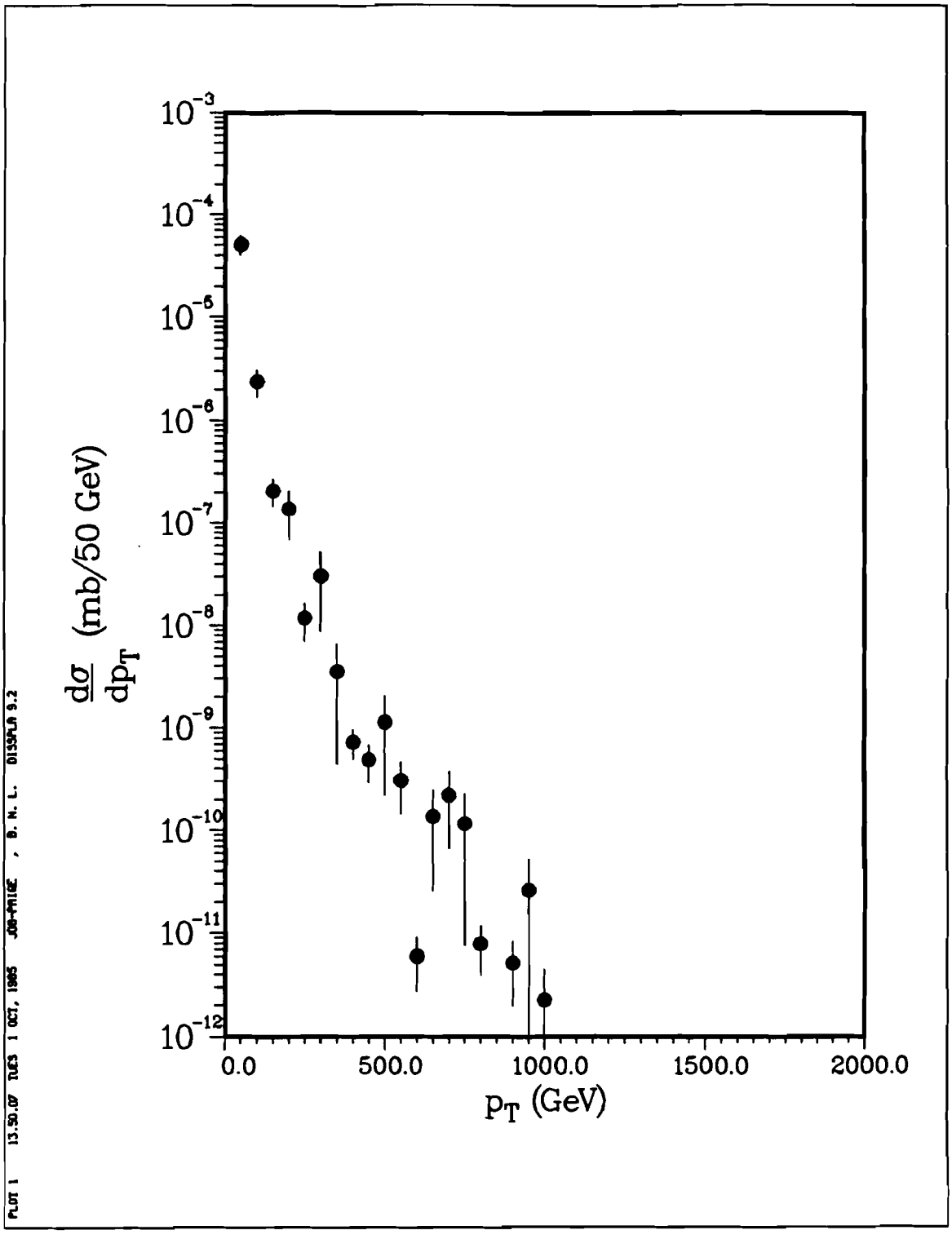

Fig. 4: Differential cross section for $e^{\pm}$ and $\mu^{\pm}$ from heavy quark semileptonic decays in QCD jets vs. p_T.

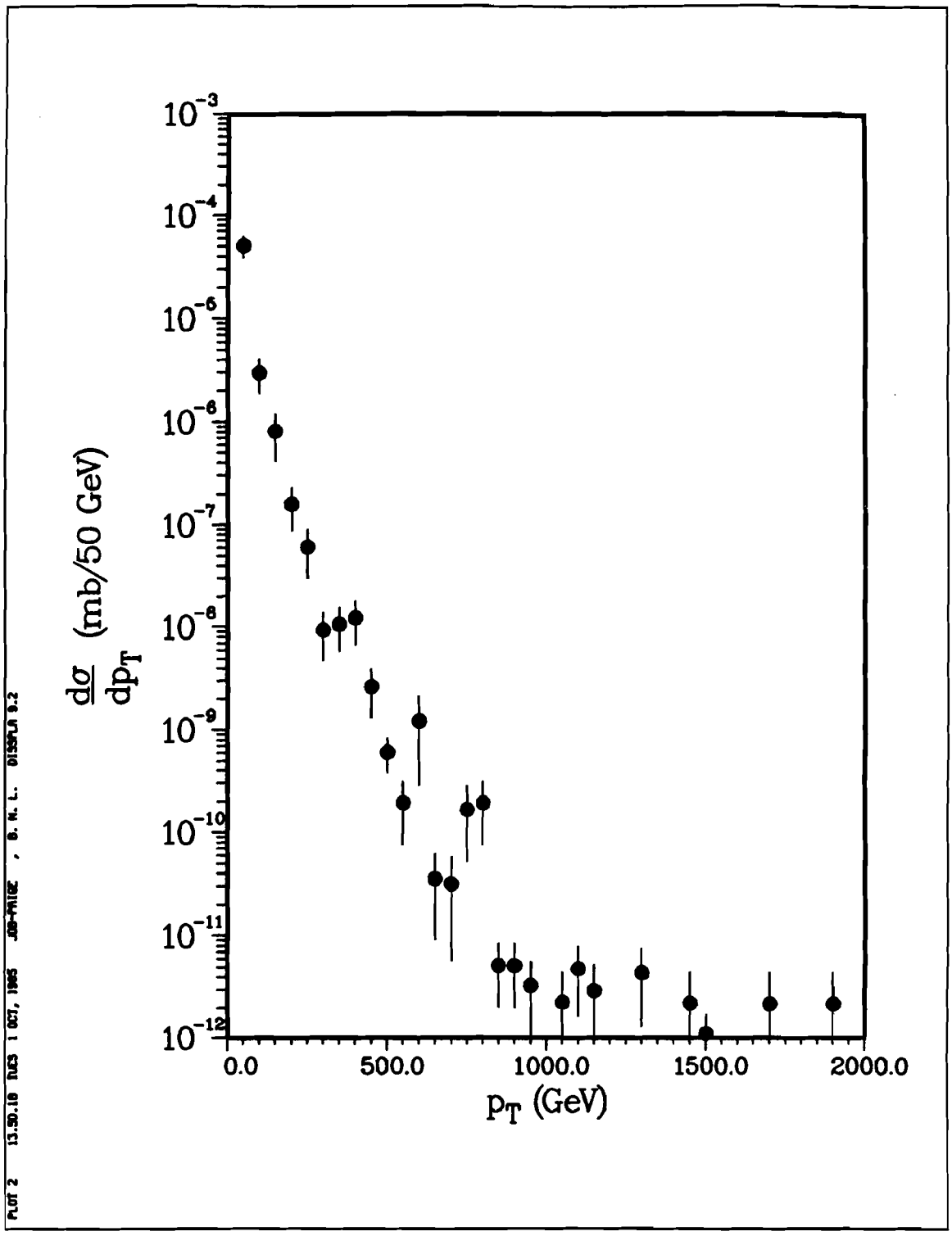

Fig. 5: **Differential cross section for neutrinos from heavy quark semileptonic decays in QCD jets vs. p_T.**

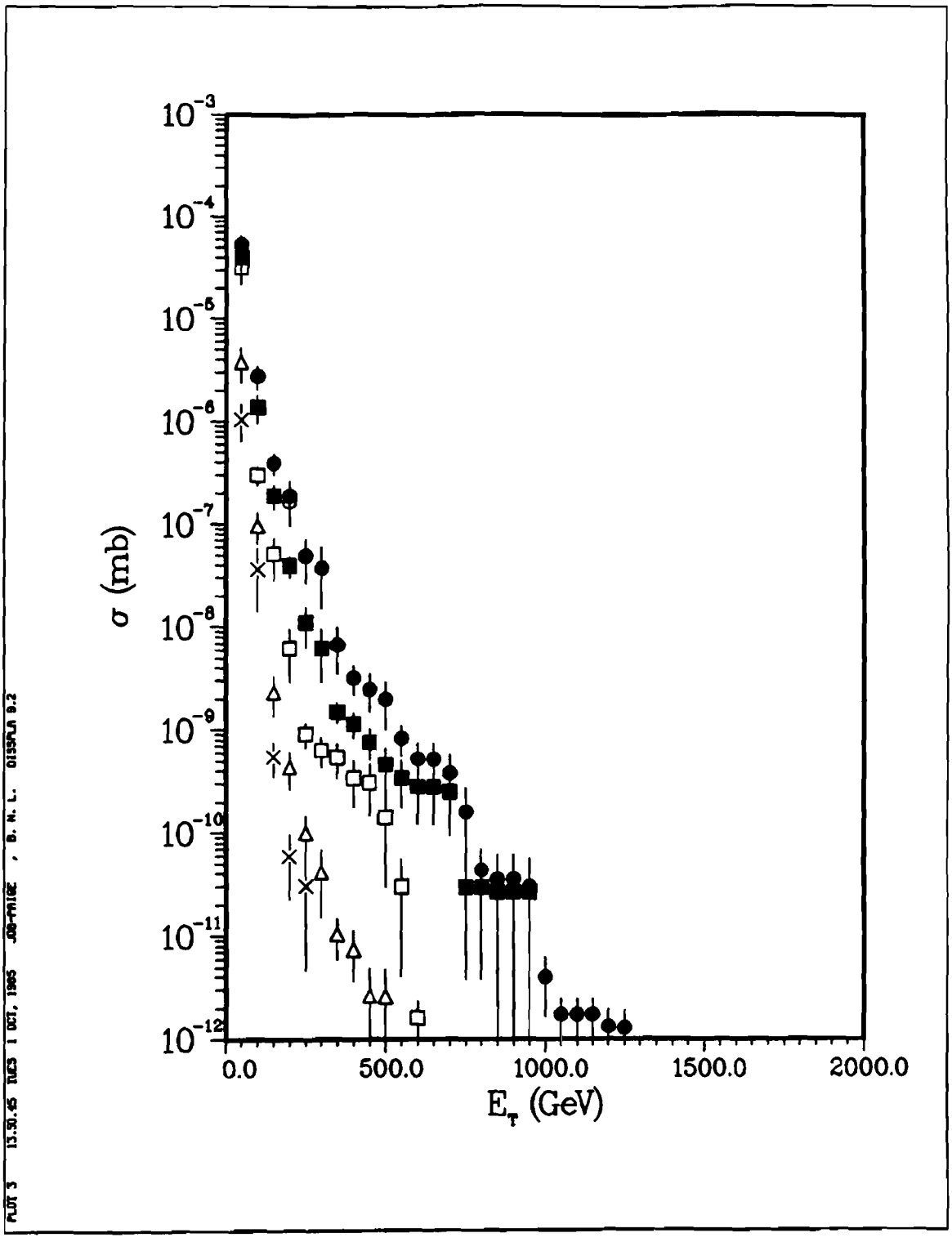

Fig. 6: Cross sections for 1, 2, 3, 4, 5, and 6 jets plus an $e^{\pm}$ or a $\mu^{\pm}$ from semileptonic heavy quark decays in QCD jets vs. the minimum E_T of a jet or the lepton. A jet is defined with $\Delta R = 1.0$.

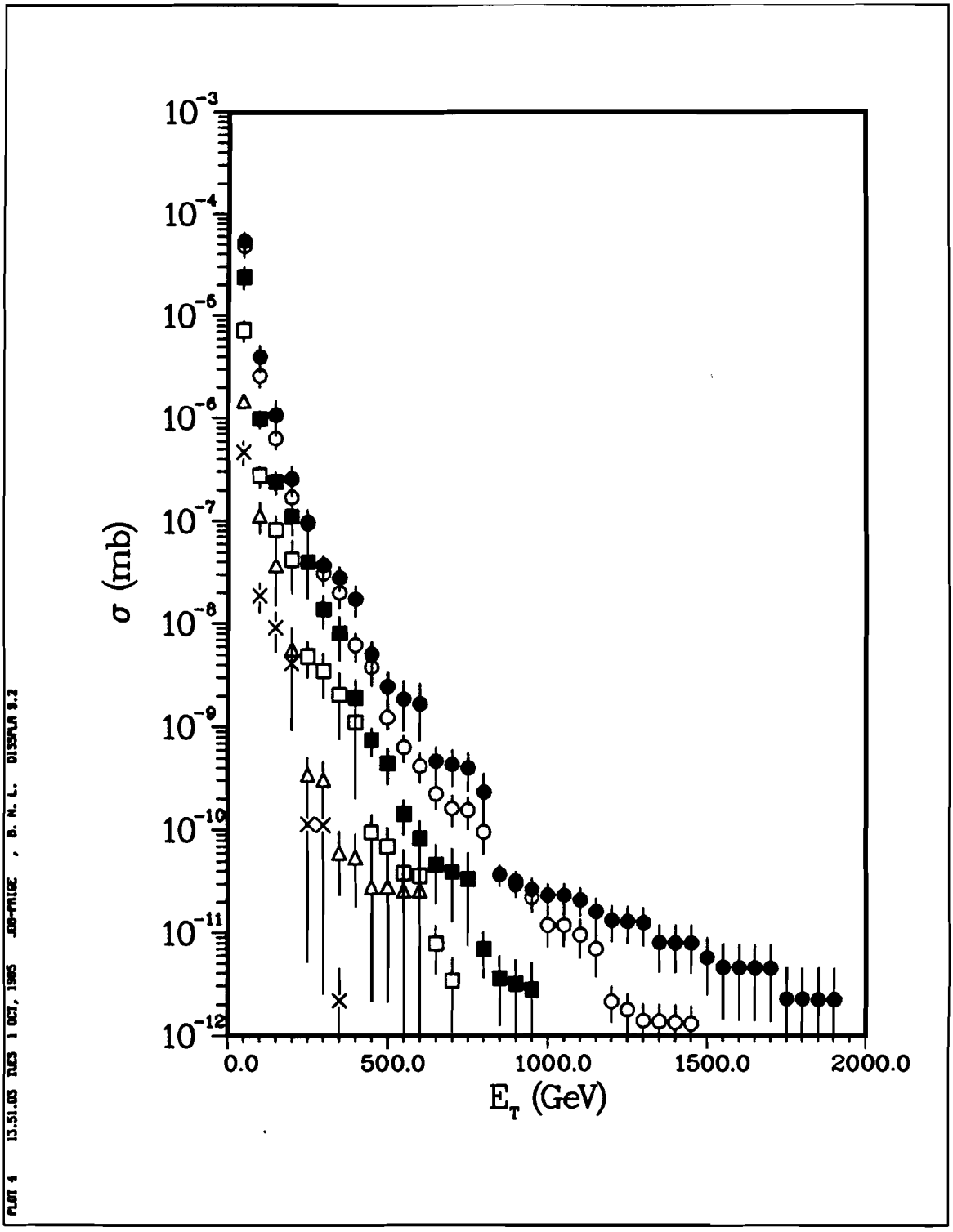

Fig. 7: Cross sections for 1, 2, 3, 4, 5, and 6 jets plus a neutrino from semileptonic heavy quark decays in QCD jets vs. the minimum E_T of a jet or the lepton. A jet is defined with $\Delta R = 1.0$.

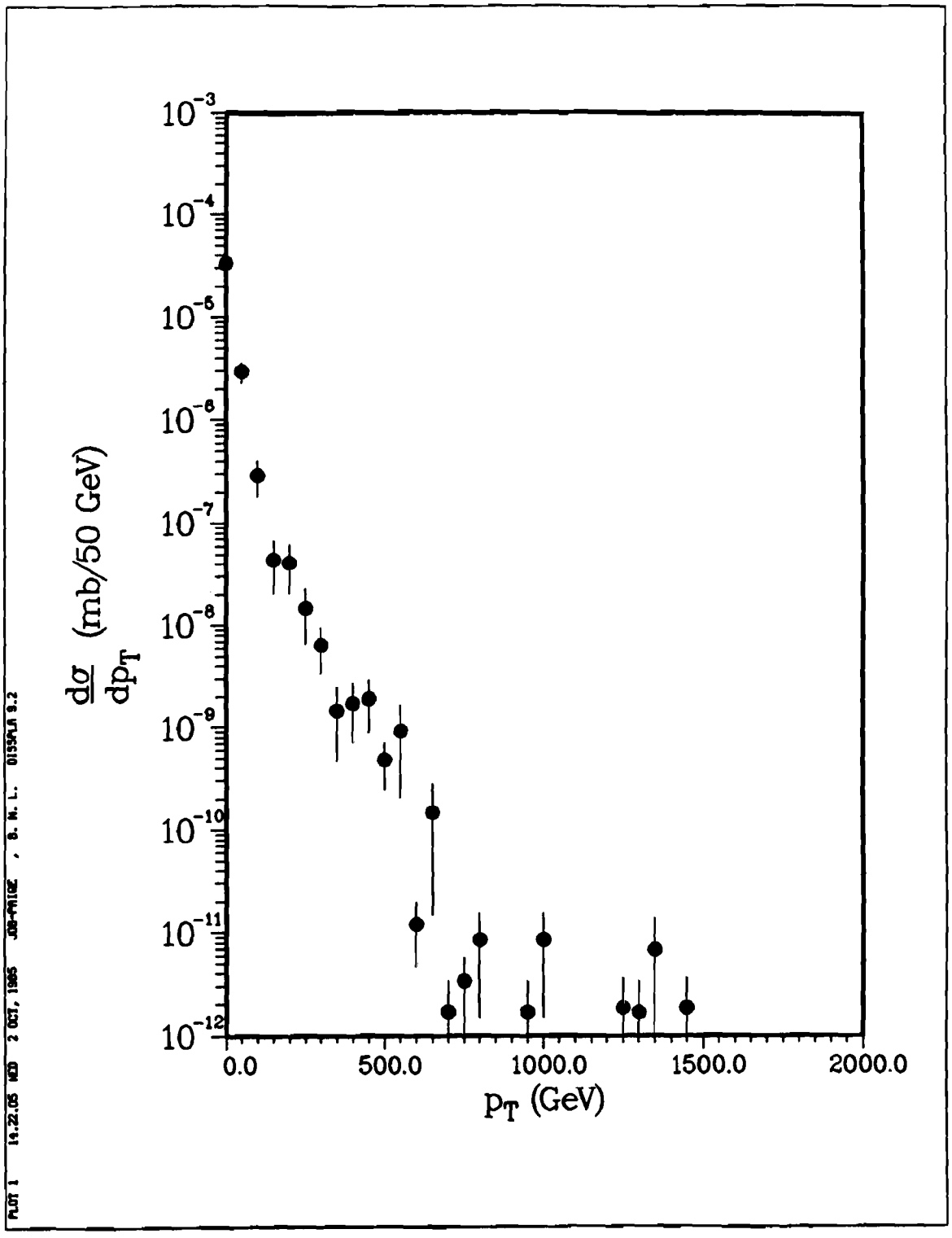

Fig. 8: Differential cross section for $e^{\pm}$ and $\mu^{\pm}$ from $W^{\pm}$ + jet events vs. p_T.

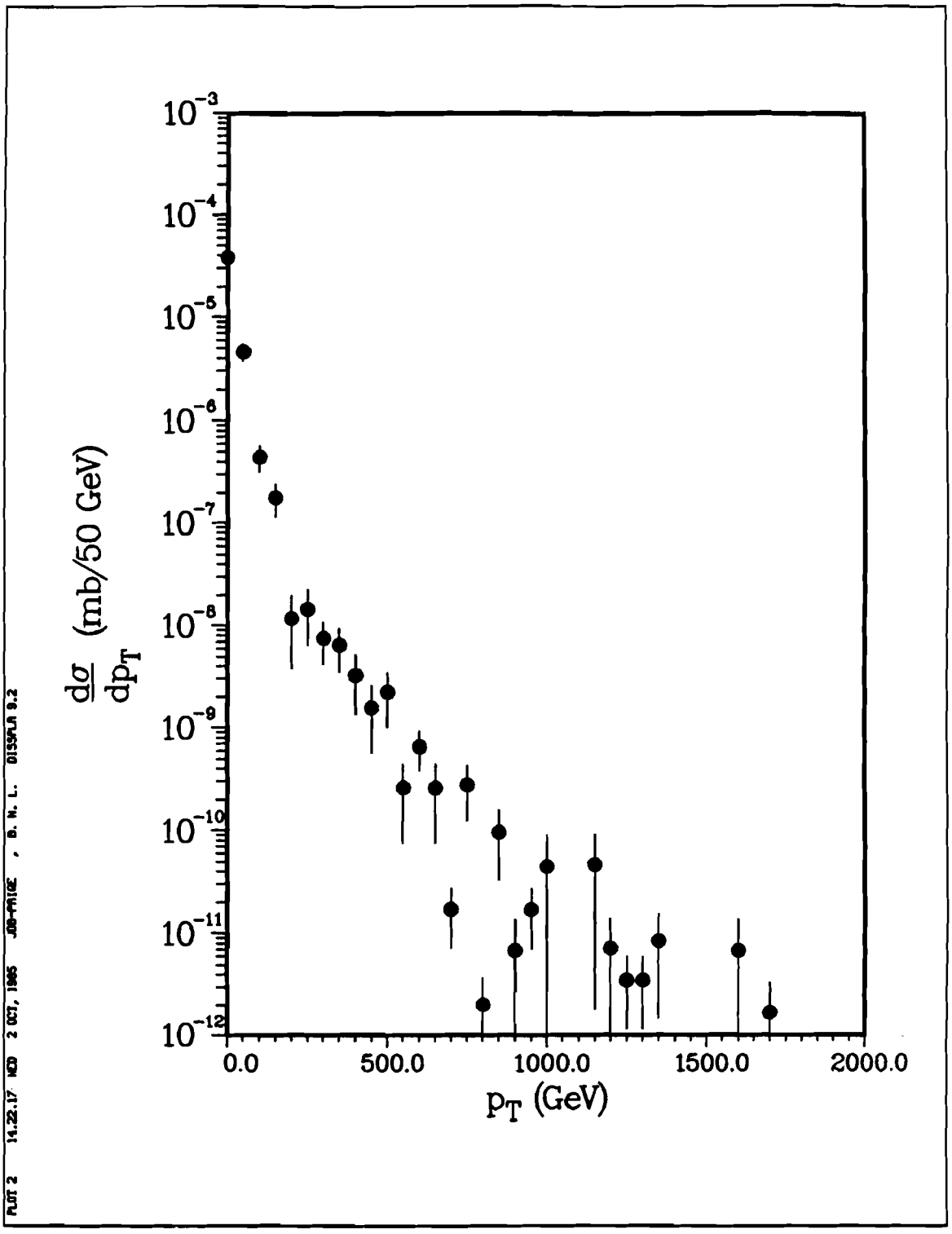

Fig. 9: Differential cross section for neutrinos from $W^{\pm}$ + jet events vs. p_T.

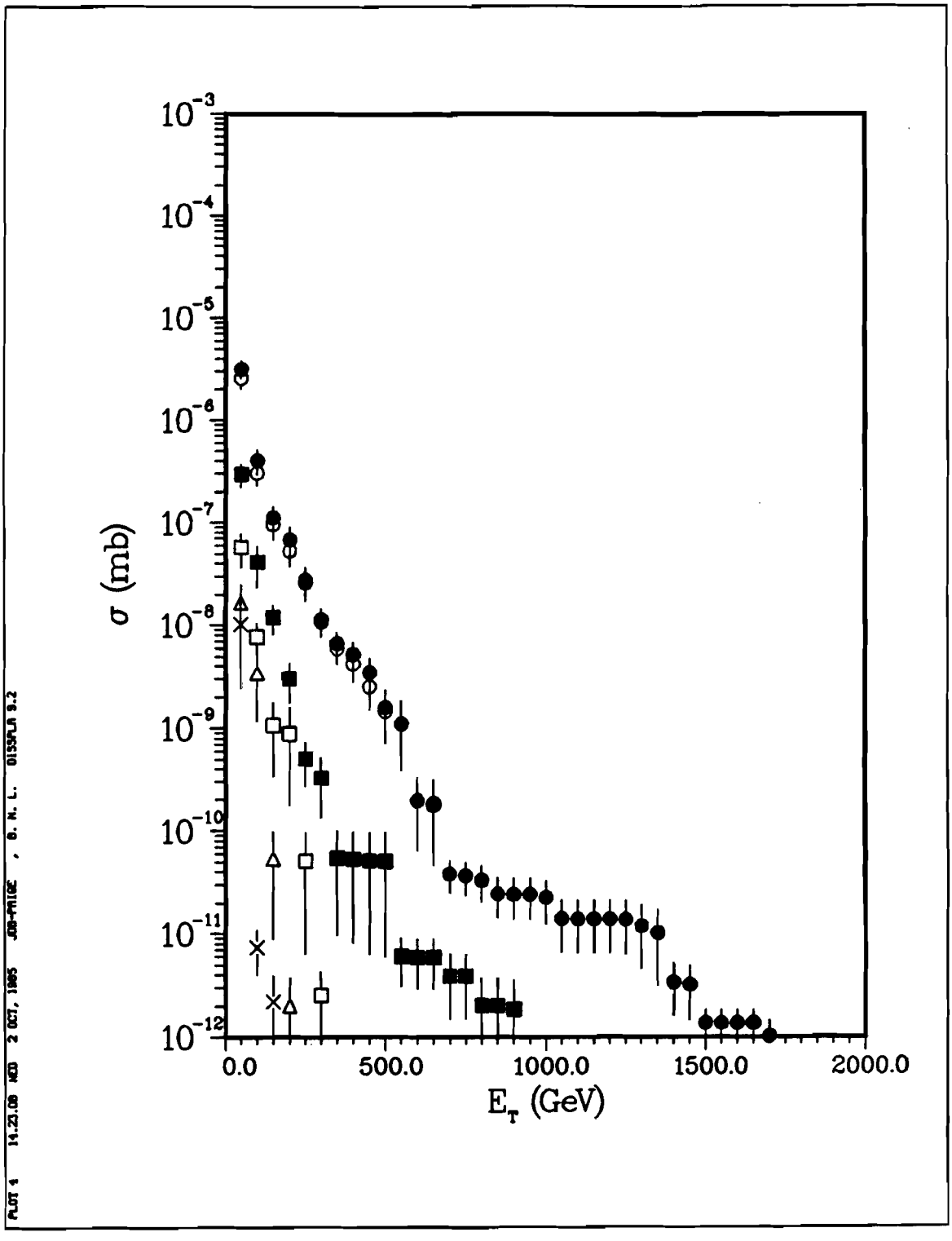

Fig. 10: Cross sections for 1, 2, 3, 4, 5, and 6 jets plus an $e^{\pm}$ or a $\mu^{\pm}$ from $W^{\pm}$ + jet events vs. the minimum E_T of a jet or the lepton. A jet is defined with $\Delta R = 1.0$.

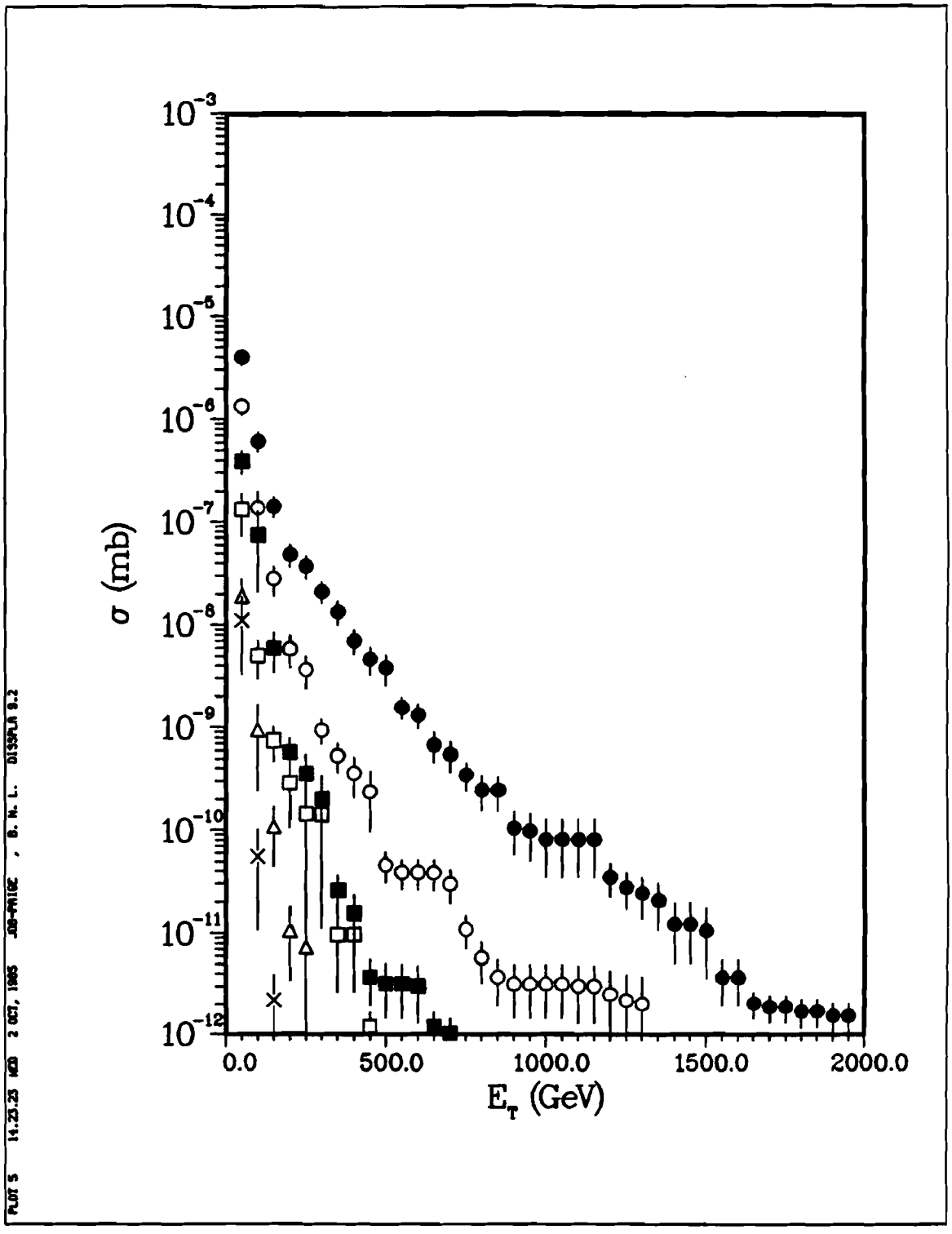

Fig. 11: Cross sections for 1, 2, 3, 4, 5, and 6 jets plus a neutrino from $W^{\pm}$ + jet events vs. the minimum E_T of a jet or the lepton. A jet is defined with $\Delta R = 1.0$.

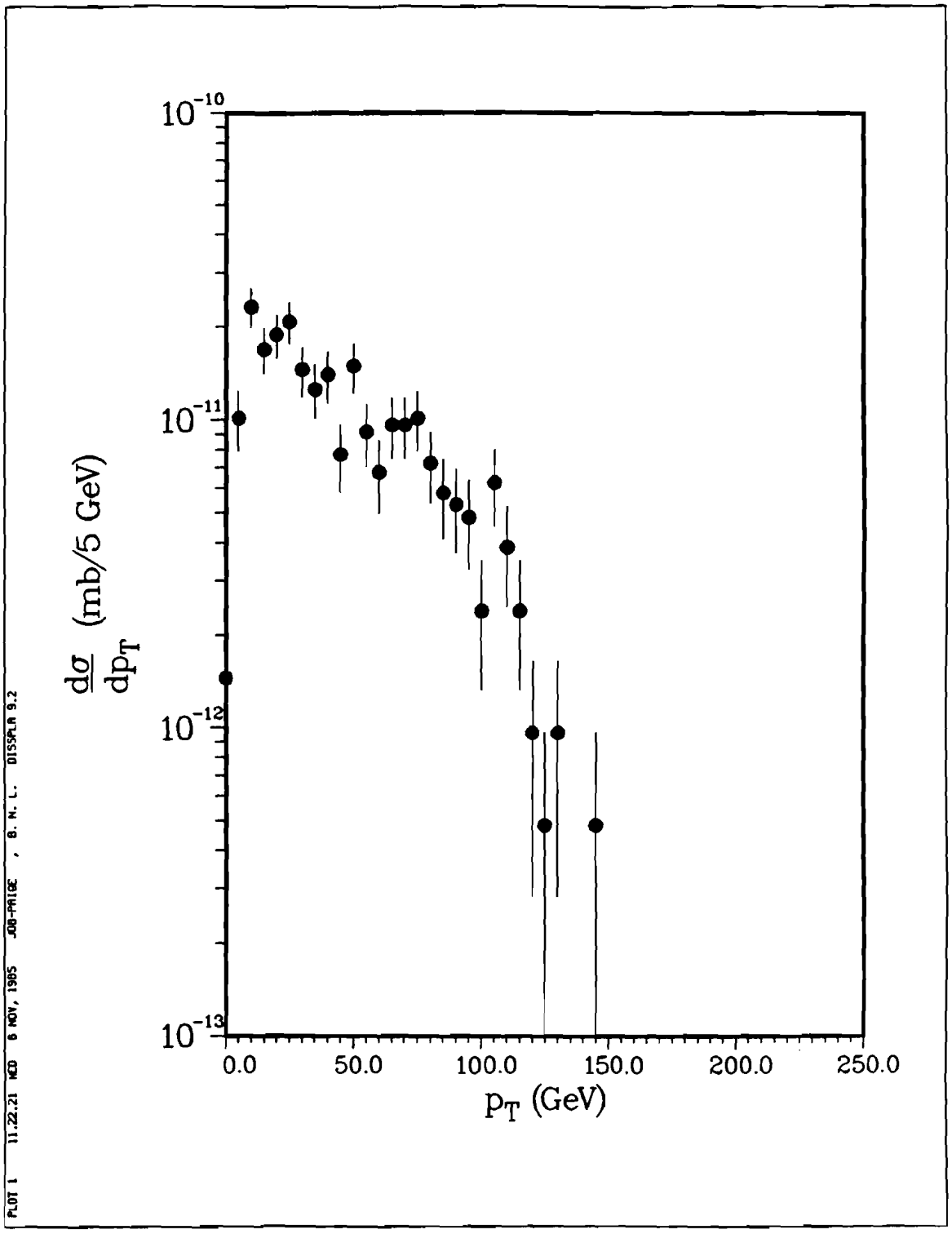

Fig. 12: Distribution of p_T for $e^{\pm}$ from $W^{\pm}W^{\mp}$ events with $p_{T,W} \approx 100\,\mathrm{GeV}$.

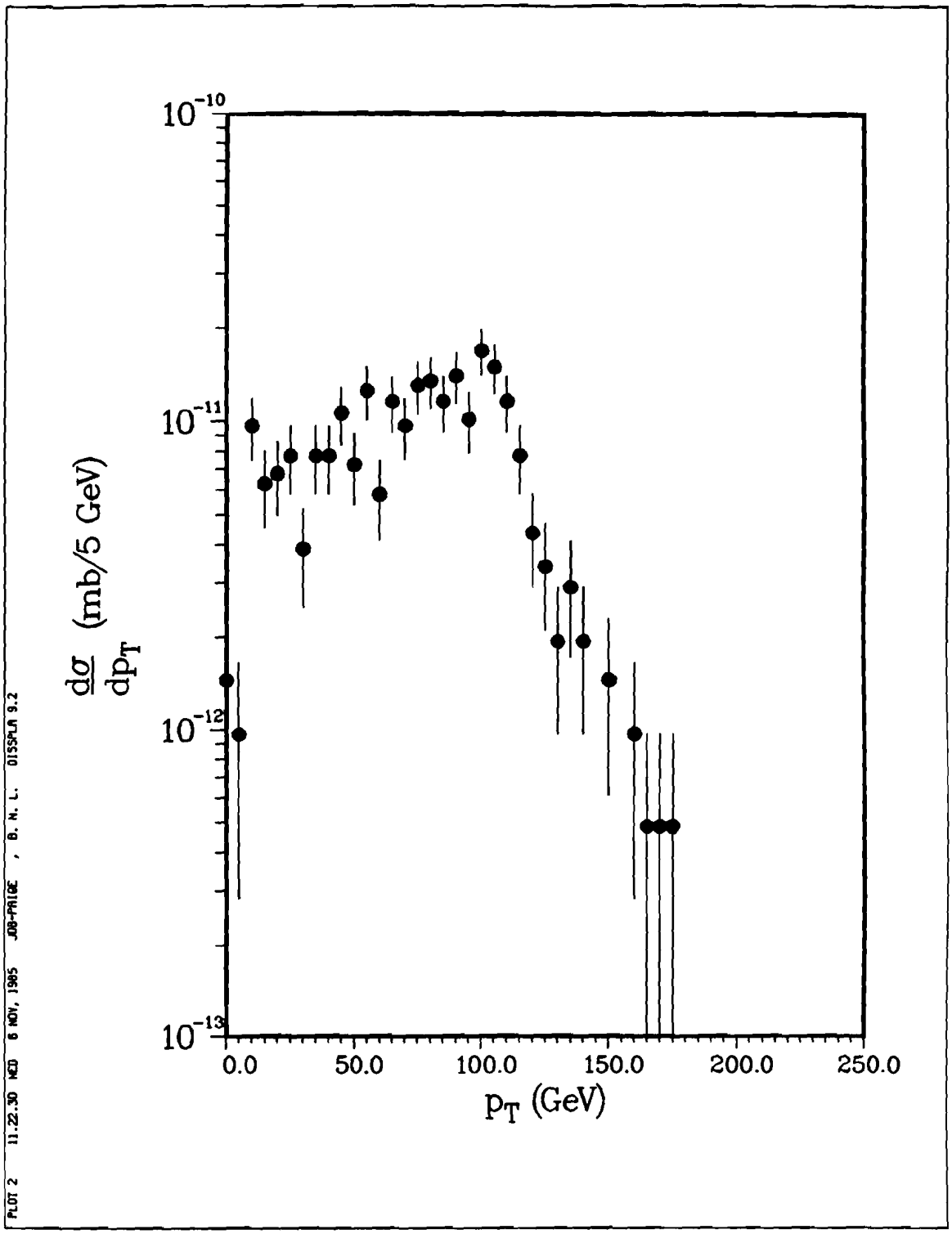

Fig. 13: Distribution of p_T for ν from $W^{\pm}W^{\mp}$ events with $p_{T,W} \approx 100\,\mathrm{GeV}$.

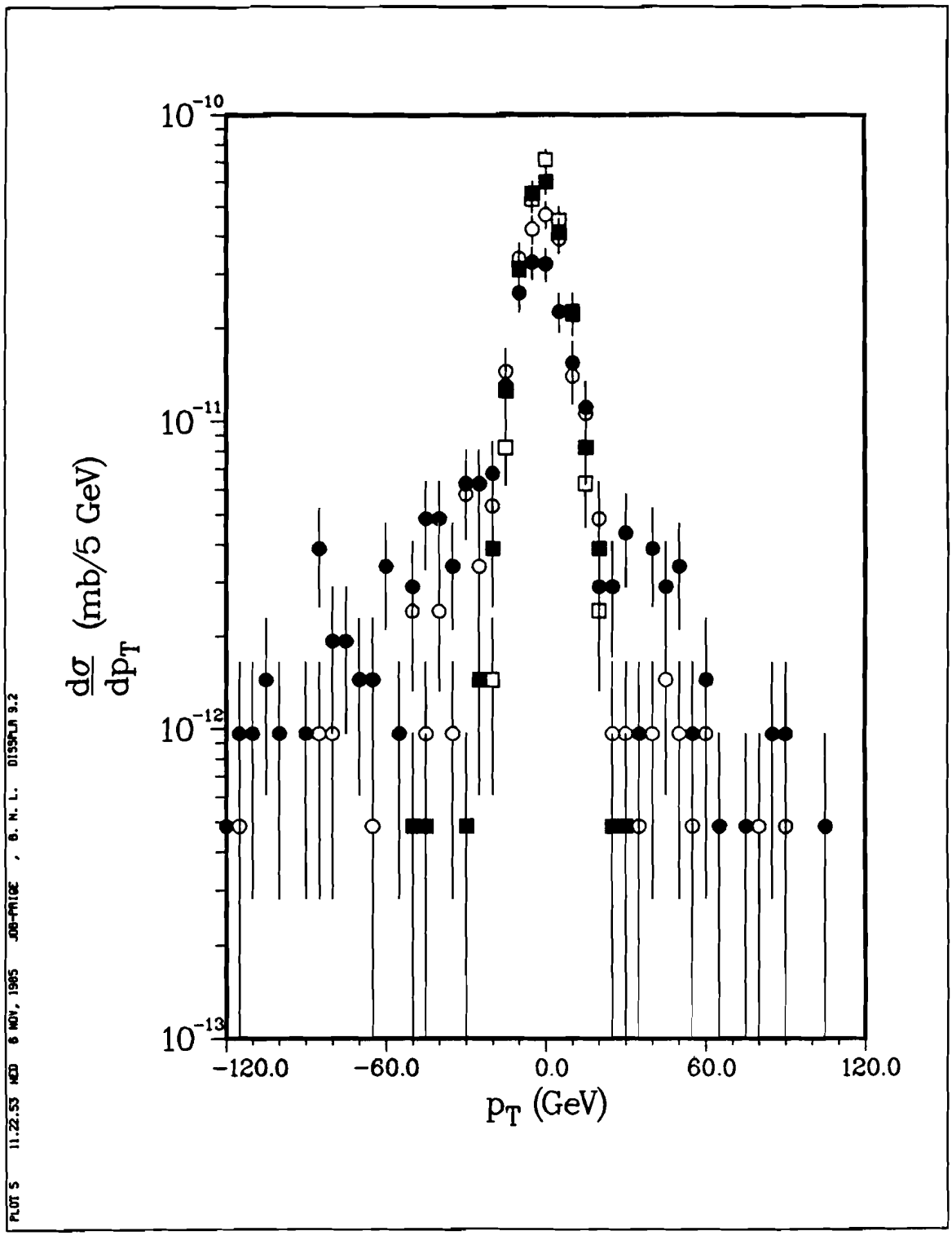

Fig. 14: Distribution of difference between actual and measured missing p_T for $W^{\pm}W^{\mp}$ events with $p_{T,W} \approx 100$ GeV for various size calorimeters: Black circles: $|y| < 3$; Open circles: $|y| < 4$; Black squares: $|y| < 5$; Open squares: $|y| < 6$.

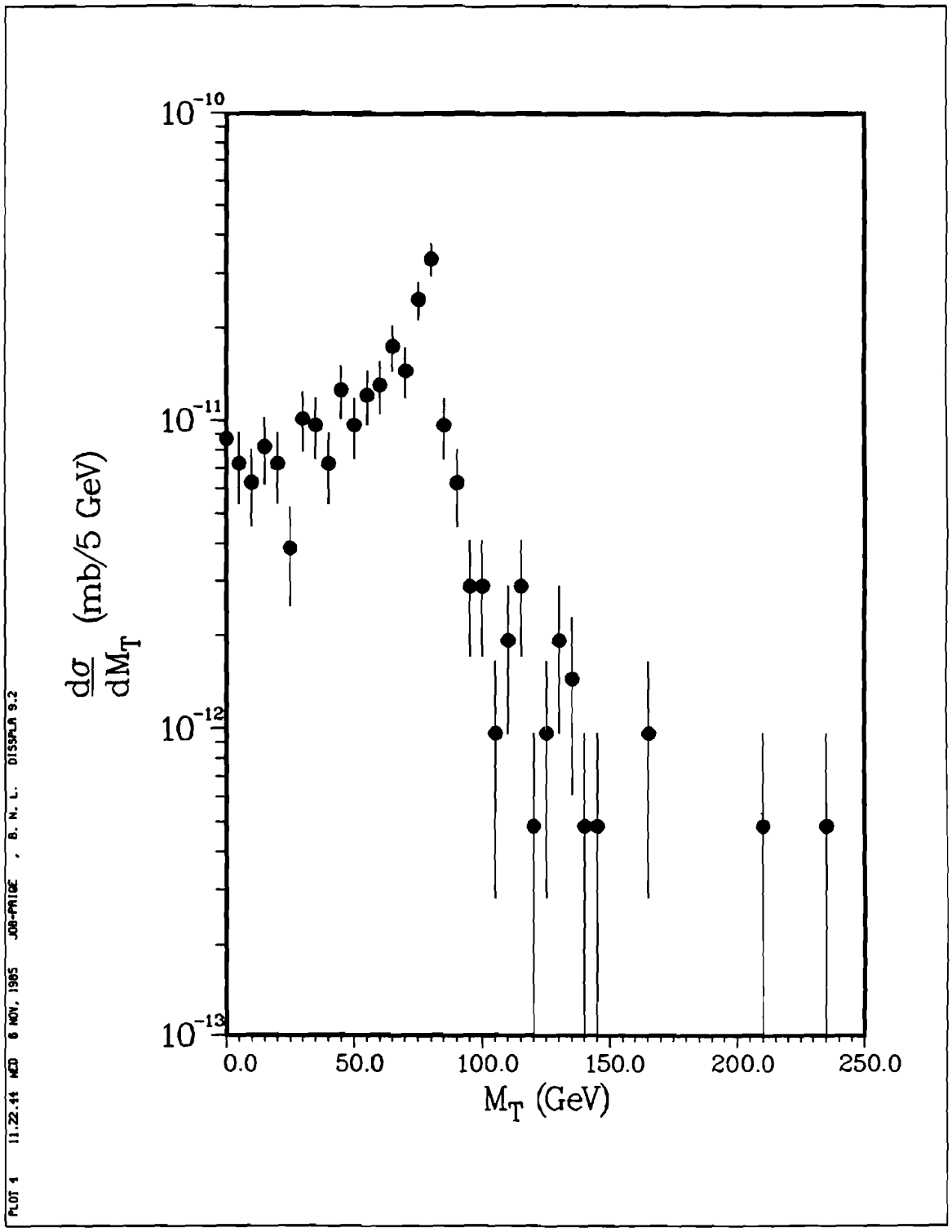

Fig. 15: Distribution of reconstructed M_T from $W^{\pm}W^{\mp}$ events with $p_{T,W} \approx 100\,\mathrm{GeV}$.

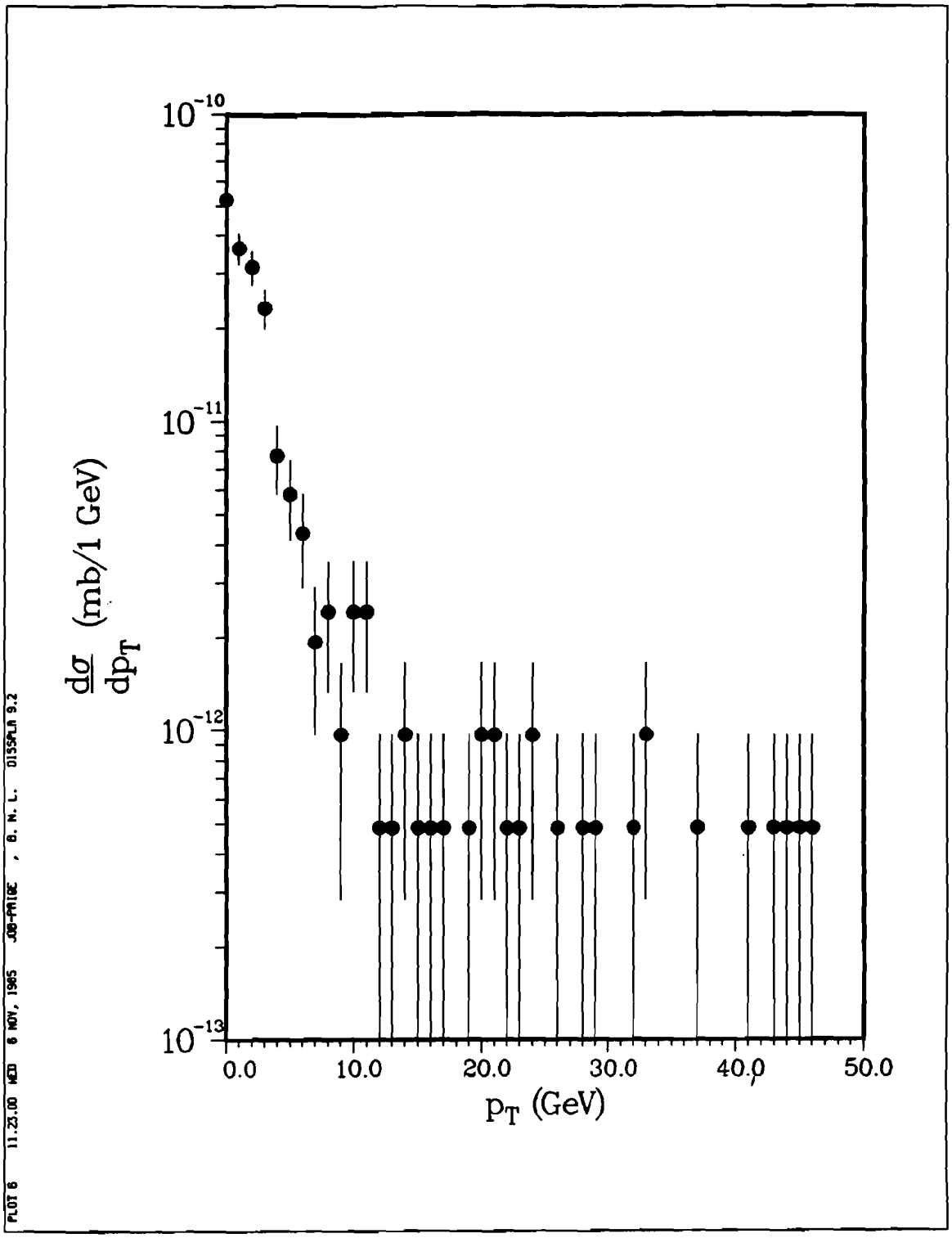

Fig. 16: Distribution of extra p_T within $\Delta R < .5$ of the $e^{\pm}$ from $W^{\pm}W^{\mp}$ events with $p_{T,W} \approx 100\,\mathrm{GeV}$.

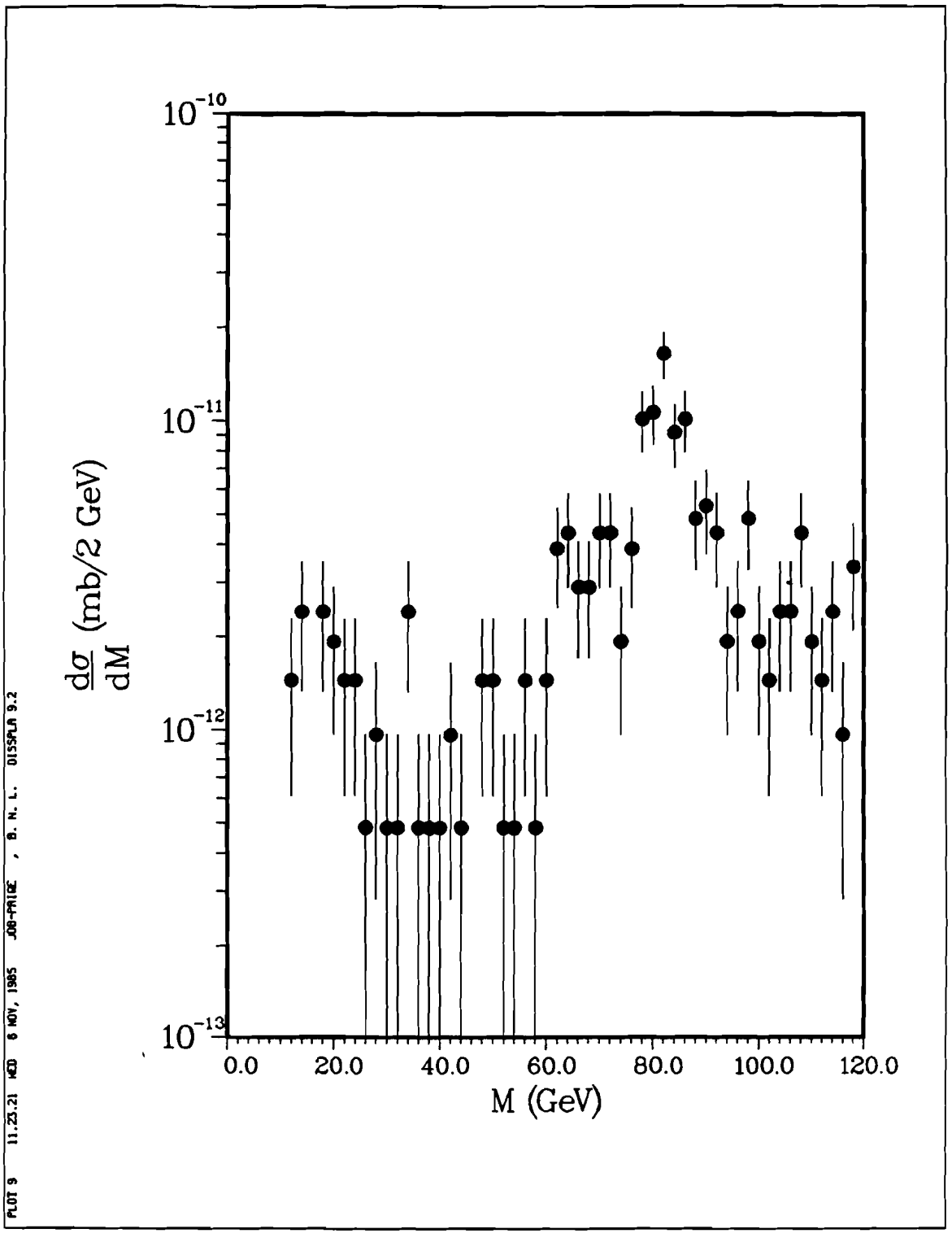

Fig. 17: Distribution of reconstructed $W^{\mp} \to \bar{q}q'$ mass for $W^{\pm}W^{\mp}$ events with $p_{T,W} \approx$ 100 GeV.

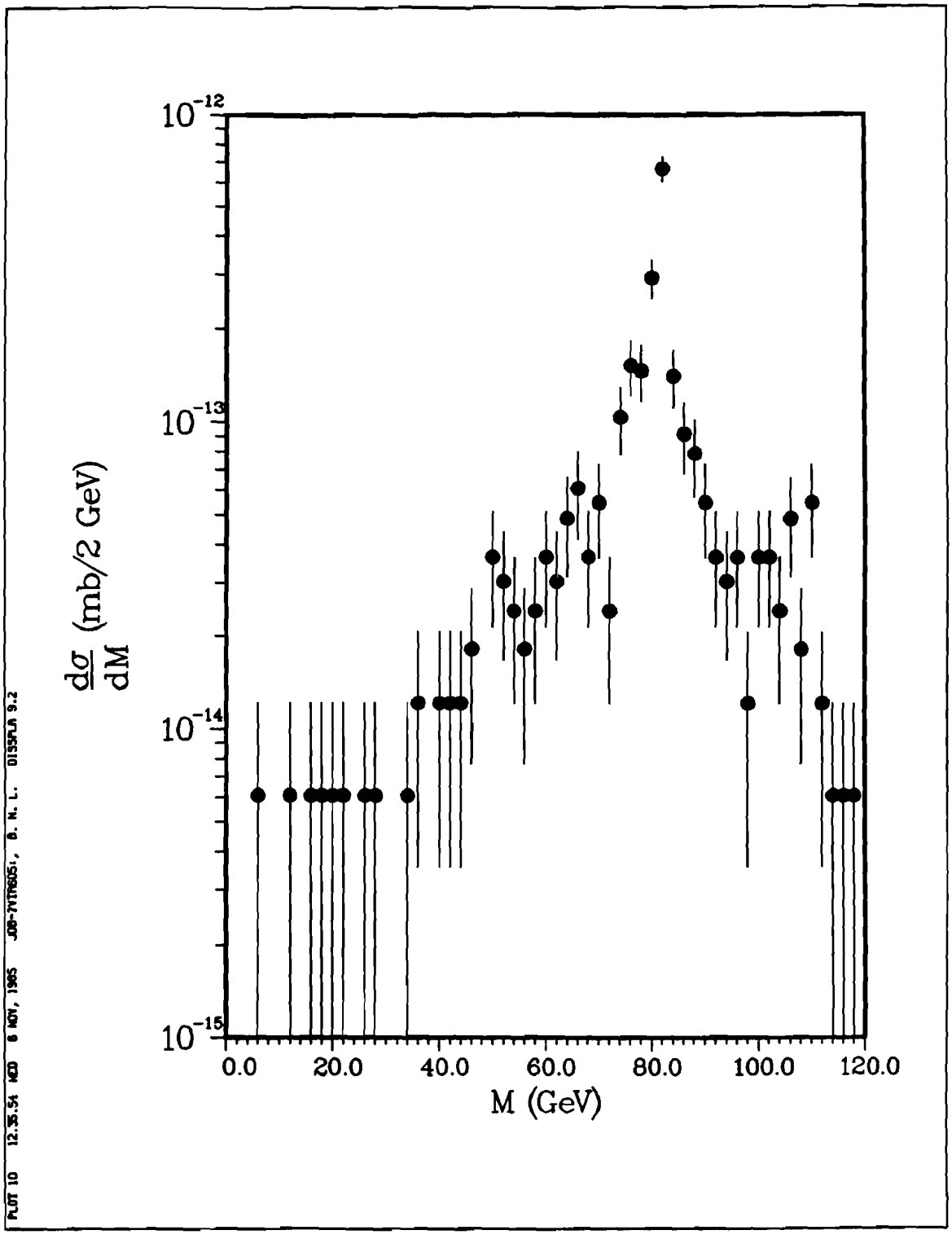

Fig. 18: Distribution of reconstructed $W^{\mp} \to \bar{q}q'$ mass for $W^{\pm}W^{\mp}$ events with $p_{T,W} \approx$ 500 GeV.

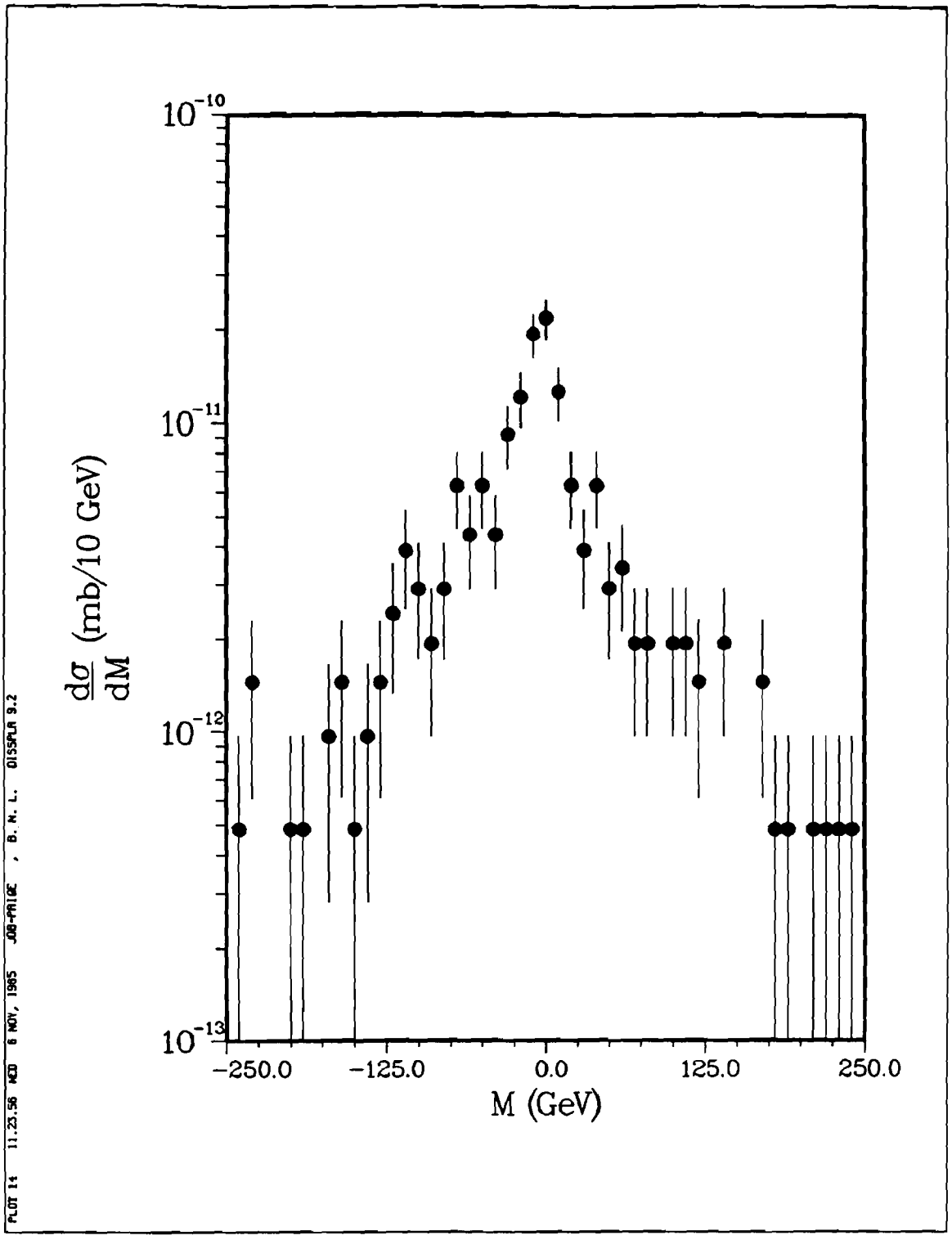

Fig. 19: Distribution of reconstructed $W^{\pm}W^{\mp}$ mass for $W^{\pm}W^{\mp}$ events with $p_{T,W} \approx$ 100 GeV.

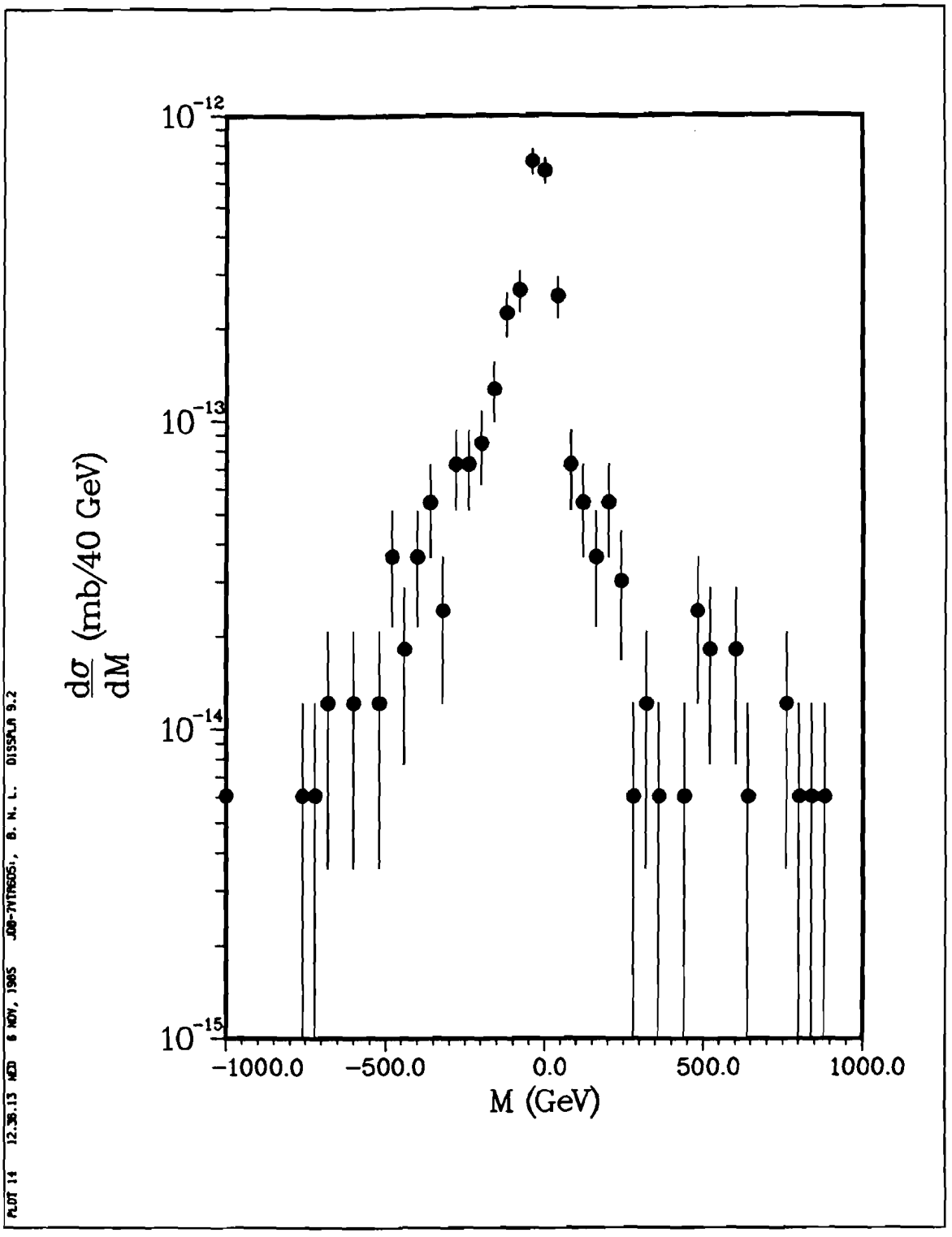

Fig. 20: Distribution of reconstructed $W^{\pm}W^{\mp}$ mass for $W^{\pm}W^{\mp}$ events with $p_{T,W} \approx$ 500 GeV.